SMiRT-12 / K. Kussmaul (Editor)
1993 Elsevier Science Publishers B.V.

E09/2

THE EFFECT OF THERMAL LOADS ON BUCKLING STRENGTH OF CYLINDRICAL SHELLS

Y. Kawamoto[1], T. Kodama[2] and S. Matsuura[3]

[1]Nagasaki Research and Development Ctr, Mitsubishi Heavy Industries Ltd., Nagasaki, Japan
[2]Kobe Engine Works and Shipyard, Mitsubishi Heavy Industries Ltd., Kobe, Japan
[3]Central Research Institute of Electric Power Industry, Chiba, Japan

1. INTRODUCTION

Nuclear power plant components must be designed taking account of strong seismic loads in countries with frequent earthquakes like Japan. When designing such thin-walled shell components as a main vessel of a fast breeder reactor(FBR),one should consider the possibility that buckling might occur.

In Japan, a series of buckling research has been conducted under contract with the Ministry of International Trade and Industry to develop the aseismic design method for a demonstration FBR. This study has been also done as a part of them.

The problem of thermal loads on buckling strength is one of the important problems in the buckling research for FBR because axial temperature gradient is produced in a main vessel and the significant thermal stress is induced at the level of sodium as shown in Fig.1. Some studies on the effect of thermal loads on buckling strength were carried out (Brochard,1987), (Nakamura, 1987), but its effect in the actual vessel has not been evaluated quantitatively. We have already reported the effect of thermal loads on buckling strength of a pool-type reactor vessel. (Kawamoto,1989)

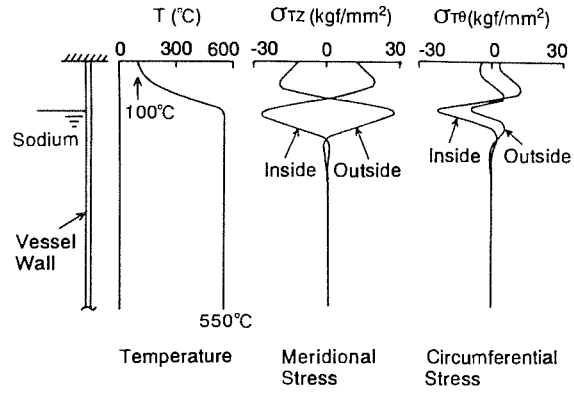

Fig.1 Thermal stresses near the sodium level of a loop-type vessel.

In this paper, we focus on a loop-type reactor vessel and investigate the effect of thermal loads accompanying with axial temperature change near the sodium level. And the reduction of buckling strength due to the thermal loads is quantitatively evaluated.

2. BUCKLING TESTS

2.1 Test Condition and Test Setup

The effect of thermal loads is caused by the interaction between the thermal

factors and the buckling mode as shown in Fig.2. Therefore, the test condition should be selected so that the thermal factors and the buckling mode in the model are similar to those in an actual vessel. We carried out 2 buckling tests varying the thermal condition. The test conditions are given in Table 1.

The models have the similar nondimensional shape parameters (R/t, L/R) to an actual vessel. Each model was fabricated by rolling an austenitic stainless steel plate into a cylindrical form and welding together the rolled plate edges longitudinally. No stress relief was carried out. The dimensions and initial deflection of the models were carefully measured and then the maximum amplitude of initial radial deflection in each model was less than 0.2 mm except near the welding line.

Next, the test setup is shown in Fig.3. The temperature distribution with steep gradient of over 25 °C/mm was produced in model 1 using high frequency induction heat coils to simulate the thermal effect of an actual vessel. The measured temperature distribution is shown in Fig.4. The maximum thermal stress in the lower part of model 1 is estimated on linear calculation as follows:
the meridional bending stress is approximately 45 kgf/mm^2, the circumferential compressive membrane stress is approximately -15 kgf/mm^2 and the circumferential bending stress is approximately 10 kgf/mm^2. On the other hand, the uniform high temperature distribution of approximately 550 °C was produced into model 2 as shown in Fig. 4.

Table 1. Dimensions of models and test conditions.

Model	Material		Dimensions				Thermal Cond.	
	Type	$\sigma_{0.2}$ (kgf/mm^2)	Diameter D (mm)	Length L (mm)	Thickness t (mm)	Height H (mm)	Tmax (℃)	Thermal Distribution
1	SUS304	17.3	320	240	1.40	320	550	with gradient
2	SUS304	17.3	320	240	1.40	320	550	uniform

where $\sigma_{0.2}$ is 0.2% proof stress at 550℃

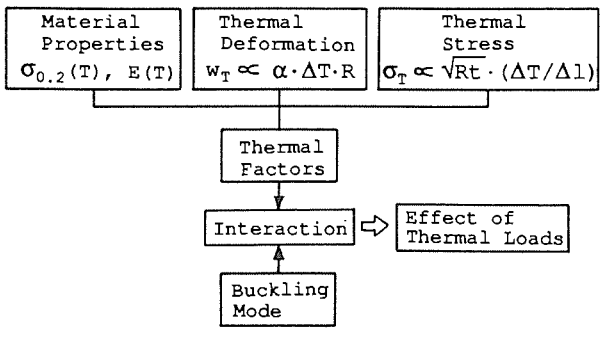

Fig.2 The factors of thermal loads.

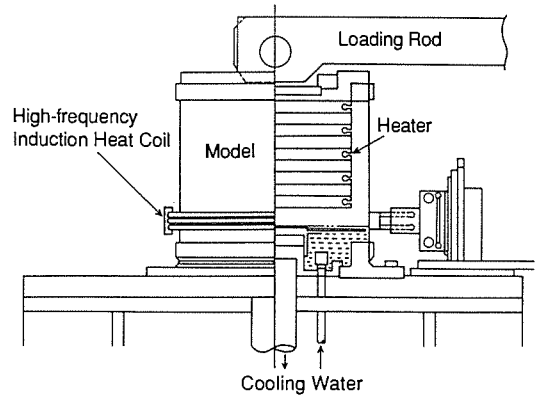

Fig.3 Test setup

2.2 Test Results

After the thermal condition was set stationary, the transverse load was applied at a point 320 mm apart from the base of the vertically cantilevered model using a screw jack. We measured the transverse load(Q), the horizontal displacement(δ) and the radial deformation(w) of the model. The summary of the test results is given in Table 2.

The buckling load(Qcr) of model 1 with steep temperature gradient was slightly larger than that of model 2 with uniform high temperature distribution. The relation between the transverse load and the horizontal displacement of model 1 is shown in Fig.5. The load carrying capacity doesn't decrease suddenly in the post-buckling region and it remains 65% of the buckling load when the displacement reaches three times as large as the buckling displacement(δcr).

Table 2. Experimental and calculated results of the test models.

Model	Experiment			Simulation		
	Max.Load Qcr(tonf)	Disp.at Qcr δcr(mm)	Qcr Q0	Max.Load Qcr(tonf)	Disp.at Qcr δcr(mm)	Qcr(Cal) Qcr(Exp)
1	6.95	1.39	1.13	6.92	1.58	0.996
2	6.66	1.39	1.07	----	----	----

where Qo is the bending yielding load, $Qo = \pi R^2 t \sigma_{0.2}/H$

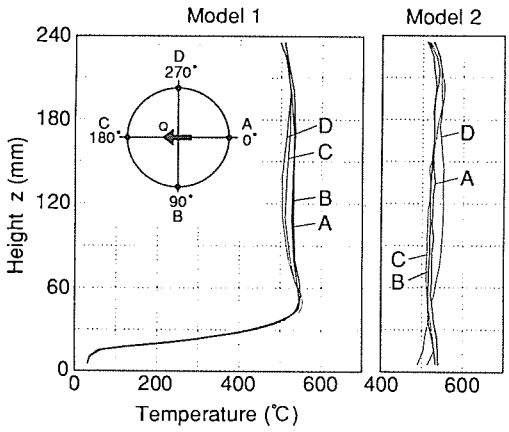

Fig.4 Temperature distribution

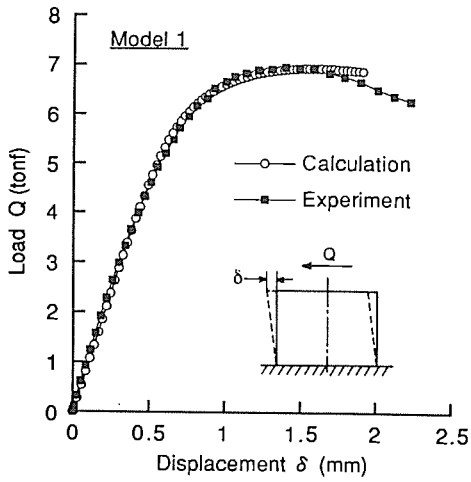

Fig.5 Load-displacement curves of Model 1 with temperature gradient.

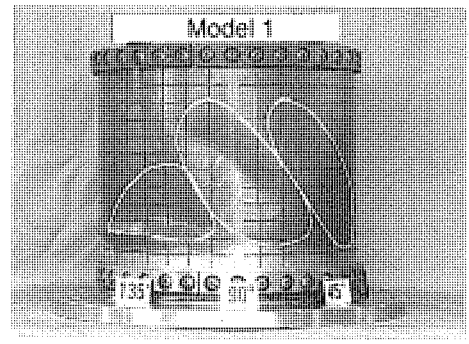

Fig.6 The buckled model (Model 1)

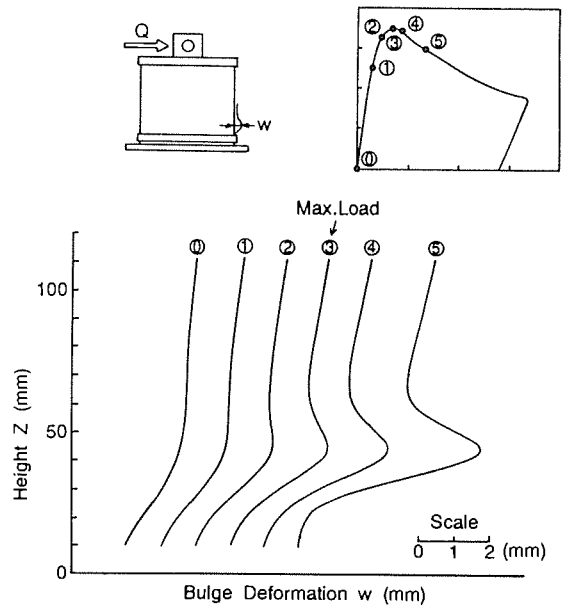

Fig.7 The growth of bulge deformation.

The bulge deformation appeared at the lower part of model in compression side due to bending and then diagonal buckles by shearing subsequently occurred at the side wall. The buckles in model 1 are shown in Fig.6. As shown in Fig.6, the buckles in model 1 occur in the high temperature region and the effective length of it seems to be slightly shorter. The growth of bulge buckling deformation along 180° line of Model 1 is shown in Fig.7. A slight deformation appears before the applied load reaches the maximum load. Once the displacement goes beyond the maximum load point, the buckling deformation increases rapidly.

2.3 Simulation of Tests

In order to verify the ability of a simulation code to simulate the buckling behavior, a numerical simulation of the buckling test of Model 1 was conducted using a nonlinear finite element analysis code,FINAS(1989 PNC) which has been developed by the Power Reactor and Nuclear Fuel Development Corporation in Japan. We selected a 4-node shell element QFLA4RT which considers shear strain distribution in element plane and Taylor series expansion in strain components(Liu, 1986).

The analytical conditions such as the dimensions of the model, the material properties and the temperature distribution were determined in the same manner as the experimental conditions. The initial deflection was reproduced according to the measured initial deflection.

The calculated result is summarized in Table 2 and Fig.5 shows the load-displacement curve of Model 1 comparing with the experimental result. The calculated buckling load agrees with the experimental one very well and the accuracy of numerical simulation was validated.

3. BUCKLING ANALYSIS OF A FULL-SCALE VESSEL

3.1 Analytical Condition

As shown in Fig.2, three thermal factors conform to the different similarity rules one another. Therefore, it is difficult to estimate quantitatively the thermal effect in the actual vessel only from the experimental results. So, we performed three buckling calculations of a full-scale vessel using the same code and elements as the mentioned simulation of Model 1. The conditions of the buckling calculations are given in Table 3. The thermal conditions are changed in 3 cases.

AL-1 has the uniform high temperature distribution. AL-2 and AL-3 have the same temperature distribution as the actual vessel. But the coefficient of thermal expansion (α) in AL-3 is assumed to be zero and then the thermal deformation and the thermal stress among the thermal factors are neglected.

We introduced the initial deflection having the same mode as the elastic buckling mode into the analytical model. The maximum amplitude was a half of the shell wall thickness. The transverse load which was assumed the horizontal seismic load was incrementally applied at the bottom of model after temperature was set stationary.

3.2 Calculated Results

The summary of the buckling analysis is given in Table 3 and the relations between the transverse load and the horizontal displacement are shown in Fig.8 comparing with each other.

There is little difference of the maximum loads between AL-2 and AL-3. It is obvious that the thermal effect on the buckling strength are mainly caused by the change of material properties due to temperature. The effect of

thermal stress and deformation can be disregarded.

Comparing AL-1 with AL-2, it is recognized that there is a little effect of the temperature distribution on the buckling strength. The maximum load of AL-1 with uniform high tempe-rature distribution is slightly less than that of AL-2 with the actual temperature distribution. The reduction of the buckling strength due to thermal loads is mainly caused by the change of material properties. The buckling strength of an actual vessel with severe temperature distribution can be conservatively estimated according to that of the same vessel under uniform high temperature.

Table 3. Summary of buckling analysis of a loop-type vessel.

Case	Dimensions				Thermal Condition			Result	
	D (m)	L (m)	t (mm)	H (m)	Distri-bution	Tmax (℃)	Thermal expansion coefficient	Qcr (tonf)	Qcr Qo
AL-1	10.4	8.5	50	11.5	uniform	550	not considered	4350	1.04
AL-2	10.4	8.5	50	11.5	with gradient	550	considered	4510	1.08
AL-3	10.4	8.5	50	11.5	with gradient	550	not considered	4530	1.09

where Qo is the bending yielding load, $Qo = \pi R^2 t \sigma_{0.2}/H$

Next, the buckling deformation and the equivalent membrane stress distribution of AL-2 are shown in Fig.9. The membrane stress becomes high in the bulge near the sodium level and the ridge of diagonal deformation.

In case of a loop-type reactor vessel, a bulge deformation due to bending precedes diagonal buckles due to shear. It seems at a glance that the local thermal stress and defor-mation near the sodium level interact with bulge deformation due to bending and reduce the buckling strength. But the membrane stress near the sodium level is com-pressive in the circumferential direction as shown in Fig.2. The compressive membrane stress due to temperature distribution acts to restrain yielding due to bulge deformation which produces com-pressive stress in the axial direc-tion and tensile stress in the circumferentialdirection. There-fore, there is less effect of thermal stress and defor-mation on the buckling strength as one expected at glance.

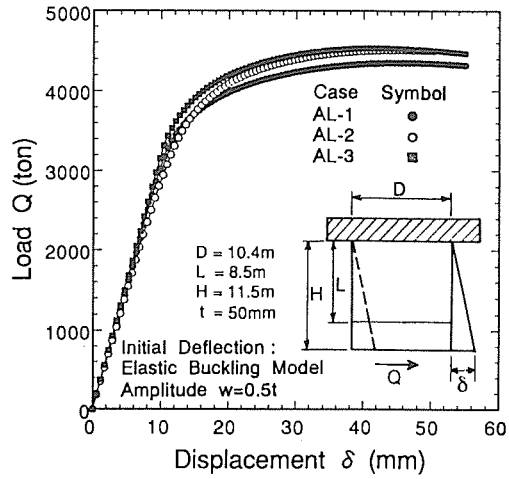

Fig.8 Load-displacement curves of a loop-type full-scale vessel.

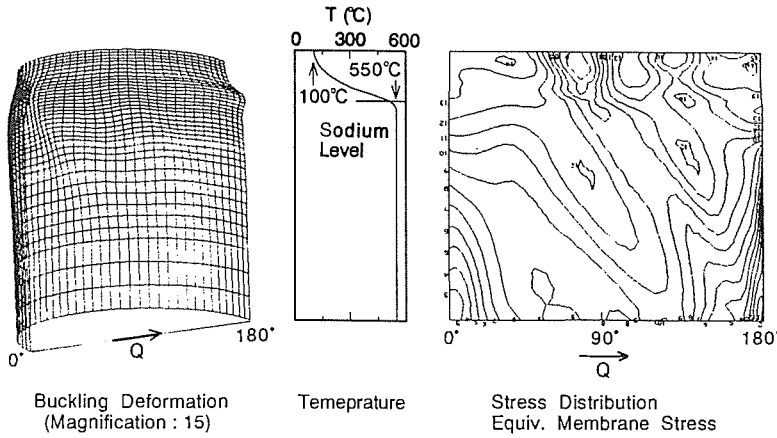

Fig.9 Buckling deformation and stress distribution.

4. CONCLUSIONS

The conclusions made from the present study are as follows:

(1) We focus on a loop-type FBR and the buckling loads of the models subjected to similar thermal loads to the actual vessel are obtained experimentally. In the test, a bulge deformation due to bending preceded diagonal buckles due to shear. And the buckling load can be estimated by nonlinear finite element analysis with sufficient accuracy.

(2) The reduction of the buckling strength due to thermal loads is mainly caused by the change of material properties. The effect of the thermal stress and deformation induced by thermal loads are not so large as one expected at glance because the compressive membrane stress near the sodium level acts to restrain yielding due to bulge deformation.

(3) The buckling strength of an actual vessel with severe temperature distribution can be conservatively estimated according to that of the same vessel under uniform high temperature in case of a loop-type vessel.

ACKNOWLEDGEMENT

This study has been carried out as a part of the project of the Ministry of International Trade and Industry, titled "Verification Tests of Fast Breeder Reactor Technology", which has been conducted since 1987. We thank Professor Hiroshi Akiyama of the University of Tokyo and members of Buckling Research Task Group for their useful discussion and suggestion very much.

REFERENCES

Brochard,J. et al. 1987. Thermal load influence on reduction of critical buckling loads. Trans. of SMiRT-9, vol. E : 209-218.

Liu,W.K. et al. 1986. Resultant-stress degenerated-shell element. Computer methods in applied mechanics and engineering, vol. 55 : 259-300.

Kawamoto,Y. et al. 1989. The effect of thermal loads on the buckling strength of a fast breeder reactor vessel. Trans. of SMiRT-10, vol.E : 251-255.

Nakamura,H. et al. 1987. Plastic buckling of short cylinders with axial temperature distribution under transverse shearing loads. Trans. of SMiRT-9. vol. E : 219-224.

Power Reactor and Nuclear Fuel Development Corporation 1989. User Manual of FINAS(Version 11.0) : PNC N9520 89-019